Applied Nanoscience (2022) 12:3835–3850
https://doi.org/10.1007/s13204-022-02530-6

ORIGINAL ARTICLE

Nano-insecticide: synthesis, characterization, and evaluation of insecticidal activity of ZnO NPs against *Spodoptera litura* and *Macrosiphum euphorbiae*

Priyanka Thakur[1] · Sapna Thakur[2] · Poonam Kumari[3] · Mamta Shandilya[4] · Sushma Sharma[5] · Peter Poczai[6,7] · Abdullah A. Alarfaj[8] · R. Z. Sayyed[9]

Received: 21 March 2022 / Accepted: 3 June 2022 / Published online: 12 July 2022

Abstract

The preliminary insecticidal efficacy of green synthesized Zinc oxide nanoparticles ZnO (NPs) against insect pests associated with tomato crops was investigated in this study, i.e., *Spodoptera litura* (Tobacco cutworm) and *Macrosiphum euphorbiae* (Potato aphid). The ZnO NPs were green synthesized using *Zingiber officinale* rhizome extract and characterized using X-ray diffraction XRD, field emission scanning electron microscopy (FESEM), energy dispersive X-ray (EDX), and high-resolution transmission electron microscopy (HR-TEM). The FE-SEM and HR-TEM analysis confirmed the surface morphology and shape of ZnO NPs. The FTIR spectrum study revealed the numerous functional groups in the ZnO NPs, zinc acetate, and ginger extract. UV spectroscopy was used to analyze the optical peak of ZnO NPs. The effect of ZnO NPs at different concentrations (100 ppm, 200 ppm, 300 ppm, 400 ppm, and 500 ppm) was studied against insect pests associated with tomato crops, i.e., *S. litura* (Tobacco cutworm) and *M. euphorbiae* (Potato aphid). On application of ZnO NPs at different concentrations, 3rd instar larvae of *S. litura* and adults of *M. euphorbiae* showed 100% mortality @ 500 ppm ZnO NPs at the exposure period of 144 h. The results revealed that an increase in concentrations of the ZnO NPs increased the mortality in the insects. The findings demonstrated the effectiveness of green synthesized ZnO NPs as an effective control agent against insects/pests. Nanoparticles act as an eco-friendly alternative insecticide for insect/pest management compared to synthetic insecticides such as thiamethoxam and imidacloprid),

Keywords ZnO NP · XRD · FTIR · FESEM · UV · *S. litura* · *M. euphorbiae*

✉ Sushma Sharma
sushsharma1987@gmail.com

✉ Peter Poczai
peter.poczai@helsinki.fi

✉ R. Z. Sayyed
sayyedrz@gmail.com

Sapna Thakur
thakurento29@gmail.com; sapnabiotec@gmail.com

Poonam Kumari
punamnisha8789@gmail.com

Mamta Shandilya
mamta2882@gmail.com

Abdullah A. Alarfaj
aalarfajj@ksu.edu.sa

[1] Department of Entomology, DKSG Akal College of Agriculture, Eternal University, Sirmour 173101, India

[2] Department of Biotechnology, DKSG Akal College of Agriculture, Eternal University, Sirmour 173101, India

[3] Department of Physics, Akal College of Basic Sciences, Eternal University, Sirmour 173101, India

[4] School of Basic Sciences, Shoolini University, Solan 173229, India

[5] Department of Plant Pathology, DKSG Akal College of Agriculture, Eternal University, Sirmour 173101, India

[6] Finnish Museum of Natural History, University of Helsinki, PO Box 7, 00014 Helsinki, Finland

[7] Faculty of Biological and Environmental Sciences, University of Helsinki, P.O. Box 65, 00065 Helsinki, Finland

[8] Department of Botany and Microbiology, College of Science, King Saud University, P.O.Box 2455, Riyadh 11451, Saudi Arabia

[9] Department of Microbiology, PSGVP Mandal's S I Patil Arts, G B Patel Science, and STKVS Commerce College, Shahada 425409, India

Introduction

Tomato (*Solanum lycopersicum*) is one of the most important, popular, and widely distributed vegetables globally. Nowadays, many factors are responsible for the low yield of tomatoes worldwide, and insect pests are the major ones. Because of their tenderness and softness, tomatoes are more vulnerable to pest attacks than other vegetable crops. The greenhouse whitefly, *Trialeurodes vaporariorum* Westwood; the green peach aphid, *Myzus persicae*; spider mites, *Tetranychus* spp.; the potato aphid, *Macrosiphum euphorbiae* (Thomas); the noctuid, *Spodoptera litura* F.; fruit borer, *Helicoverpa armigera* and cutworm, *Agrotis segetum* are the major insect pest of tomato in the open field and protected cultivation (Sajjad et al. 2011). Excessive use of pesticides has increased insect resistance (Kranthi et al. 2001), a source of contamination, and has negative consequences for human health and other species. Finally, pesticide residues found in nature and agricultural products have sparked the development of alternative pest control methods. The various eco-friendly, biomedical properties of metal nanoparticles have been provoking desirable attention of the research community and establishing new milestones in advancement in engineered technology and research (Kapadia et al. 2021). Potent antimicrobial activities of ZnO NPs synthesized by different methods were due to their increased surface area (Thakur et al. 2020a, b; Vijayakumar et al. 2019). Nanoparticles penetrate the microbial cell wall and exhibit anti-pathogenic activity (Kapadia et al. 2021; Thakur et al. 2021; Schwartz et al. 2012). As potent insecticides, ZnO NPs can be attributed to the absorption and abrasion of the protective wax layer on the cuticle of insects, causing the insects to lose water and die from desiccation (Arumugam et al. 2016). Pathogenic contaminations are severe health concerns worldwide; manifold antibiotic resistance and lack of appropriate solutions in developing countries pose a significant threat to human health. (Sirelkhatim et al. 2015). Nanomaterials' unique properties have made them an excellent candidate for biological applications. Nanoparticles can easily bind to protein molecules due to their unique physicochemical properties (Yu et al. 2020; Sharon et al. 2010). There have been numerous studies on the toxicity effects of nanoparticles on bacteria, fungi, and animal pathogens (Nayeri et al. 2021). Still, little research has been carried out to investigate the toxicity effect of nanoparticles on insects. Antibacterial, antifungal, and photochemical properties of ZnO NPs are all possible in recent studies (Shandilya et al. 2020, Malaikozhundan et al. 2020). Recent advances in nanotechnology have opened up new possibilities in agriculture. Nanomaterials will revolutionize agriculture by developing potential and efficient pest management approaches (Rai and Ingle 2012). Traditional agricultural methods such as integrated pest control are ineffective, and chemical pesticides have adverse effects on animals and humans and lower soil fertility (Ragaei and Sabry 2014). Pesticides are not only used in agriculture; they are also used to manage household pests and insect vectors. However, they are highly toxic and pose serious health and environmental risks. Agriculture employees are exposed to these contaminants both directly and indirectly (Rani et al. 2021; Bhardwaj et al. 2021). Raafat reported biosynthesis and anti-mycotoxigenic activity of *Zingiber officinale* Roscoe-derived metal NPs such as Ag NPs, Cu NPs, and ZnO NPs, and their antifungal activities against some mycotoxigenic fungi were determined (Raafat et al. 2021). Over the past two decades, interest in the production of plant extract-assisted CuO NPs, CdS NPs, AgCl-NPs, and Cr_2O_3 NPs has evolved exponentially and increasing day by day. Many studies have illustrated the effectiveness of plant extract-assisted CuO NPs in catalytic, pharmaceutical, and environmental uses from this perspective. From this viewpoint, several metal NPs like CuO NPs, CdS NPs, AgCl-NPs, and Cr_2O_3 NPs have numerous applications in biological processes, medicine, energy devices, environmental remediation, and industrial fields from nanotechnology(Cuong et al. 2022; Dabhane et al. 2021; Ghotekar et al. 2021; Pandit et al. 2022; Kashid et al. 2022).

The plant ginger belongs to the family Zingiberaceae. It is used as a common condiment for various foods and medicinal usage in India for headaches, nausea, rheumatism, and cold. The anti-inflammatory properties of ginger have been known and valued for centuries (Jabborova et al. 2020, 2021; Janaki et al. 2015). Among reported chemical synthesis methods, green chemistry routes using plant extracts have been commonly preferred for the synthesis of ZnO NPs due to the environmentally friendly, cost-effective, and safe nature of the resulting NPs for human therapeutic use (Donmez 2020). As a result, nanotechnology has emerged as one of the most exciting new pest control methods (Bhattacharyya et al. 2010). We present our findings in this study regarding the green synthesis of ZnO NPs using the rhizome extracts of ginger and their characterization via standard analytical methods. A biological approach using powder extract of dry ginger rhizome has been used as a reducing material and a surface stabilizing agent for the synthesis of ZnO NPs. ZnO NPs synthesized using *Cannavis, Jatropha, Aloe vera,* and *Tinospora* leaves extract as a reducing agent (Thakur et al. 2021). *Averrhoa bilimbi* (L) extract is used as a reducing and capping agent for ZnO NPs green synthesis (Ramanarayanan et al. 2018).

NPs act as an alternative chemical-free method for insect pest control against *Spodoptera frugiperda* (Pittarate et al. 2021). New pest control strategies are required

by introducing substances that make them promising ''green'' alternatives to traditional pest control, and nanoparticles are one of those methods. ZnO NPs have antifungal, antibacterial, and insecticidal properties, and it has a low risk of resistance to insects. The standard characterization techniques explored the synthesized product's structure, phase, and morphology. One of the most interesting dynamically developing "green technologies" is the microwave-assisted synthesis of ZnO NPs. Compared with conventional heating, the microwave heating method has a contactless method, Volumetric heating of the feedstock, rapid energy transfer, a heating process that can be controlled with the accuracy of one second, and a green chemistry approach (Wojnarowicz et al. 2020). In different parts of the world, due to the excessive use of different insecticides, the problem of resistance has been reported. So there is a need to develop alternative approaches for solving this problem. Apart from the resistance problem in different groups of insects, the extensive use of insecticides leads to adverse effects on the ecosystem and human health. Therefore, it is the need of the hour for handling the present situation to develop alternative methods to minimize the use of insecticides. In the present study, the green synthesis of ZnO NPs using the rhizome extract of ginger and their properties, such as the surface morphologies, structures, and optical properties of samples, were analyzed. After characterization, ZnO NPs were analyzed for insecticidal efficacy against insect pests *S. litura* (Tobacco cutworm) and *M. euphorbiae* (Potato aphid). This study, therefore, sought to determine the efficacy of green synthesized ZnO nanoparticles towards *S. litura* (Tobacco cutworm) and *M. euphorbiae* (Potato aphid) under laboratory conditions.

Materials and methods

Preparation of ginger rhizome extract

Green synthesis of ZnO NPs (nanoparticles) was done using ginger rhizome extract (*Zingiber officinale)*. The healthy rhizome of the ginger plant was collected from an agriculture farm, Eternal University, Himachal Pradesh. The rhizome of ginger was washed thoroughly; its outer covering was removed from the rhizome; 10 g of rhizome was crushed and adjourned in 200 ml of double-distilled water. The prepared solution was boiled for up to 10 min at 100 °C in a glass flask. Filter the rhizome extract using Whatman filter paper; the filtrate obtained contains the metabolites and bioactive components leached from the ginger rhizome.

Synthesis and purification of ZnO NPs

Zinc acetate ($Zn(CH_3CO_2)_2$), Sigma Aldrich (99%) were purchased, and 100 ml (0.02 M) solution was made in double-distilled water. Drop by drop, zinc acetate solution was added to 100 mL of rhizome extract and stirred for 10 min on a magnetic stirrer. pH 11 was adjusted, and the final solution was exposed to room temperature. The solution was set aside for 2 h to settle the nanoparticles. The ZnO NPs were then concentrated by repetitive centrifugation and re-suspension using a cold centrifuge [Eppendorf; Model-R5210] for 15 min at 14,000 rpm. The pellet was washed and re-dispersed thrice in double distilled water to make ZnO NPs free from biochemical constituents. The green synthesized material is endorsed for drying in a hot air oven at 60 °C for 5 h. After drying, the synthesized material was annealed for 2 h at 400 °C to get a white powder as an end product for further characterization (Kausar et al. 2016). The flow chart of green synthesis of ZnO NPs using ginger rhizome extract is given in Scheme 1.

Characterization of ZnO NPs

X-Ray Diffraction (XRD, PW3040 Philips X-Ray Diffractometer); Using an XRD pattern with CuK radiation (=0.15406 nm), the structural properties were investigated. Field emission-scanning electron microscopy (FE-SEM, Model name MAIA3 TESCAN) and energy dispersive X-ray spectroscopy (Thermo Noran system SIX, PAU, Punjab) were used to examine these samples' morphology and elemental analysis. The spectral range of 4000–400 cm^{-1} was used to test ZnO NPs using a Bruker Tensor FTIR spectrometer (Shoolini University, Solan, India). HR-TEM measurements were performed on a Philips CM 200 instrument with a 200 kV accelerating voltage (Panjab University, Chandigarh, India). The optical property of ZnO NPs was analyzed using ultraviolet–visible spectroscopy (UV–Vis) (Model- Shimadzu UV 1800) in the wavelength range of 300–500 nm.

Maintenance of the laboratory culture of S. litura

The larvae of *S. litura* were collected from farmer's fields and maintained under controlled conditions in the culture room of the Department of Entomology, Eternal University; at 25 ± 10 ℃, and relative humidity was 70%. The newly emerged adults were kept in plastic jars (30 ml) with a muslin cloth covering. Adults were given a 10% sugar solution in a cotton swab to encourage egg-laying. Larvae that emerged from the eggs after 3 to 5 days were reared at 26 °C. Fresh leaves of castor and cabbage were given as food to the newly hatched feeding larvae up to the completion of the second instar. Cabbage and castor leaves changed daily. The larvae

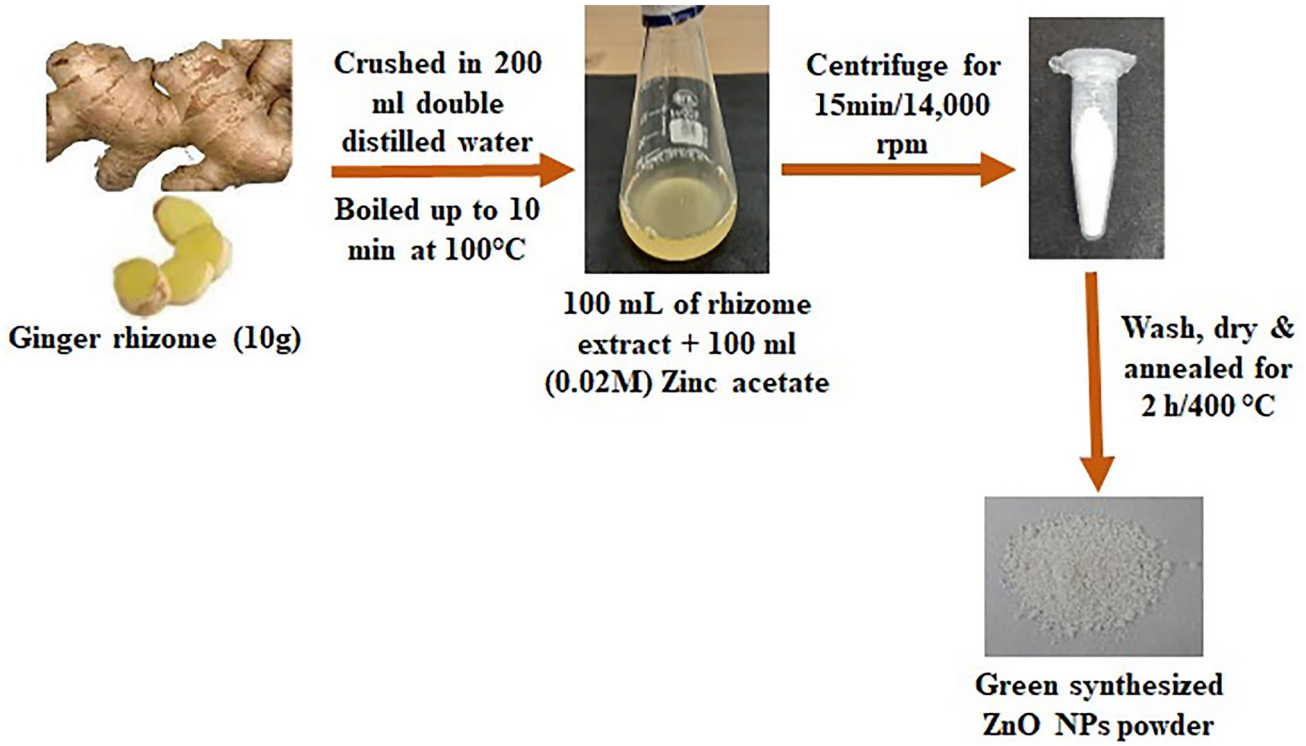

Scheme 1 Flow chart of green synthesis of ZnO NP using ginger rhizome extract

separated during the second instar, and 10–15 larvae were reared in a jar of 18 × 15 cm sealed with a muslin cloth to complete the third instar larvae. Third, instar larvae from laboratory culture were used for various experiments.

Maintenance of the laboratory culture of *M. euphorbiae*

Laboratory colonies of potato aphid, *M. euphorbiae* developed from nymphs and adults collected from the farmer's field and maintained under controlled conditions in the Department of Entomology's culture room, Eternal University temperature of 25 °C and relative humidity of 70% (RH). The nymphs and adults were separated and transferred to the Petri plates using a fine camel-hair paintbrush. They were continuously provided with fresh cabbage leaves 1–2 times per day for further experiment.

Bioassay studies on *S. litura* and *M. euphorbiae*

Effect of ZnO NP on larvae of *S. litura* and adults of *M. euphorbiae* determined by contact toxicity assay at five doses @ 100 ppm, 200 ppm, 300 ppm, 400 ppm, and 500 ppm of the nanoparticles. The experiment was carried out in a fully randomized design with three replications. Zinc oxide (ZnO) nanoparticles are thoroughly mixed with water and ready for use. After that, the insects were topically treated with fine camel-hair paintbrushes. Ten larvae of *S. litura* each in three replications were kept for all the treatment and control. Castor leaves are continuously provided to the larvae daily. For *M. Euphorbiae*, the adults of potato aphids topically sprayed with the help of a hand sprayer. Three replications per treatment were kept having 30 aphids in each treatment with control. The Petri plates having treated and untreated insects were held separately at the proper temperature and humidity 16L:8D photoperiod, and mortality was observed after 24, 48, 72, 96, 120, and 144 h.

Statistical analysis

The data were recorded and subjected to statistical analysis to determine the results' significance. Mortality data were analyzed by using Abbott's formula (Abbott 1925).

$$\text{Corrected \% mortality} = \frac{\text{\% mortality in treatment} - \text{\% mortality in the control}}{100 - \text{\% mortality in the control}} \times 100$$

The corrected % mortality data were analyzed using a Completely Randomized Design (CRD) factorial.

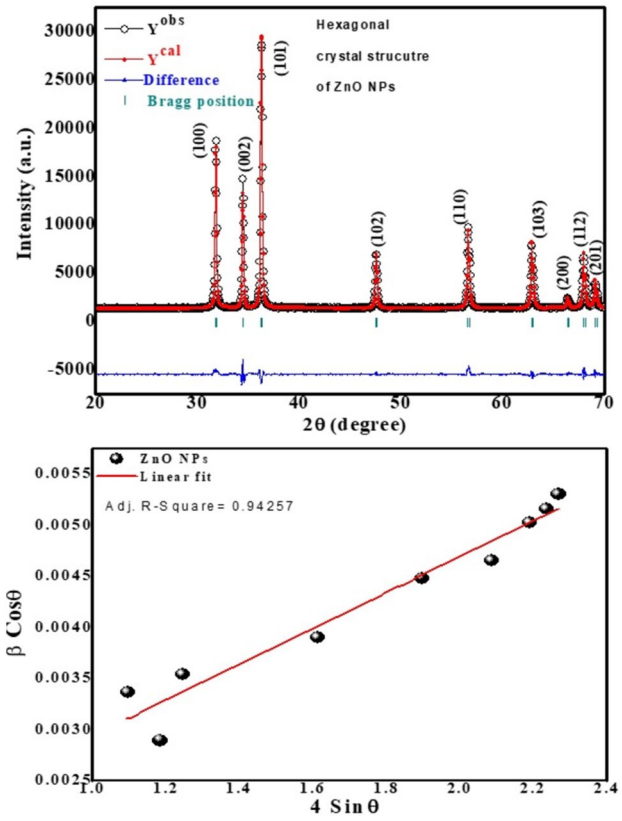

Fig. 1 XRD pattern of ZnO NP: **a** Rietveld refinement. (inset): Hexagonal crystal structure of ZnO NP and **b** Williamson–Hall (W–H) plot of ZnO NP

Results and discussion

X-ray diffraction (XRD) analysis

The XRD patterns for ZnO NPs prepared by green synthesis at room temperature are shown in Fig. 1. The XRD spectrum shows well-defined diffraction peaks corresponding to the planes (100), (002), (101), (102), and (110) that fit the JCPDS card No. 751526. Figure 1 shows the Rietveld refined XRD patterns of synthesized ZnO NPs. The observed XRD patterns are represented by the black-colored hollow circles in the fitted curves, while the solid red circles represent the calculated XRD patterns. The Bragg positions are represented by the blue vertical line, while the horizontal line represents the difference between the measured and observed patterns. A Rietveld refinement analysis was conducted using two variables (scale part and complete B-factor), one instrumental parameter (zero correction), background parameters, lattice parameters, three FWHM parameters (u, v, w), positional coordinates (x, y, z), and isotropic thermal parameters (Biso, Occ). The refined parameters, including the lattice constant, unit cell length, profile residual factor (Rp), weighted profile residual error (Rwp), predicted pattern factor (Rexp), and goodness of fit, are mentioned in Table 1. As evidenced by the lowest R-values and goodness of fit, the observed XRD pattern was well balanced by the derived pattern for ZnO NPs fit (2). According to the Rietveld refinement, ZnO NPs have a hexagonal wurtzite structure and the space category P63mc. The peak strength of the 101 plane indicates that the sample's crystallinity and crystallite size is measured from the peak width of the 101 plane by taking the full width at half limit (FWHM).

$$\text{Scherrer equation } t = \frac{0.9\lambda}{\beta \operatorname{Cos} \theta_B}$$

which is used to determine various characteristics of the crystalline material where t is the crystal size, λ is the X-ray wavelength, θ is the Braggs angle in radians, and β is the full width at half maximum the peak in radians (Kumari et al. 2015). The lattice strain and crystallite size can also be calculated by using the Williamson–Hall (W–H) method to measure the XRD peak broadening (Rai et al. 2015), as seen in Eq. (1). The Williamson–Hall method takes into account both size-induced and strain-induced broadening.

$$\beta \operatorname{Cos} \theta = \frac{K.A}{D} + 4\varepsilon \operatorname{Sin} \theta \quad (1)$$

Figure 1 demonstrates a linear association between β Cos θ and 4sin θ, and the intercept and slope of the linear fit were used to calculate the value of lattice strain and crystallite size, respectively. It also discovered that ZnO NPs have a positive lattice strain, suggesting tensile strength in the crystal structure. The strain (ε) is believed to be uniform in all crystallographic directions.

Fourier transform infrared (FTIR) spectroscopy analysis

FTIR spectroscopy is used to analyse the functional groups and bonding present in the materials and also used to identify the compositional element of the prepared samples. In Fig. 1a spectra of prepared ZnO nanoparticles (NPs) showed the band for various functional groups located at 510, 554, 1204, 1307, 15,574, 1633, 2370, 3676, 3748 cm^{-1}. The adsorption band at 3676–3748 cm^{-1} are assigned due to hydroxyl (O–H)groups stretching vibration, whereas the

band at 2370 cm^{-1} is assigned to the adsorbed CO_2 gas. The small peaks between 2400–3000 cm^{-1} are arise due to the presence of C-H stretching vibration of alkane groups. The peaks around in the region 1633–1554 cm^{-1} can indicates the presence of H–O-H bending vibration and also show the presence of C = O amide group. The strong adsorption band at 510 and 550 cm^{-1} are attributed to the Zn–O vibrations. In case of Fig. 1b the characteristic peak at 512 and 583 cm^{-1} to the Zn–O vibrations. The adsorption band at 624 cm^{-1} can be attributed to the acetate anions. The two characteristic band at 1311and 1517 cm^{-1} attributed to asymmetric and symmetric stretching of C = O bond in acetate group. The adsorption band between 3176–3351 cm^{-1} is associated with the stretching mode of water.

In Fig. 2 FTIR spectrum of ginger powder show several adsorption bands which can be assigned for hydroxyl group (3305 cm^{-1}), carbonyl group of amide (1639–1925 cm^{-1}). The small peak at 1380 cm^{-1}arise due to the presence of aromatic skeletal combined with C–H. The small band at 1044 cm^{-1}attributed due to the presence of amino acid and stretching vibrations of C–C bond.

Figures 2a–c show the FTIR spectra of ZnO, Zinc acetate, and ginger powder required in 4000 to 400 cm^{-1}. FTIR spectroscopy is used to analyze the functional groups and bonding present in the materials and identify the compositional element of the prepared samples. In Fig. 2a spectra of prepared ZnO nanoparticles (NPs) showed the band for various functional groups located at 510, 554, 1204, 1307, 15,574, 1633, 2370, 3676, 3748 cm^{-1}. The absorption bands at 3676–3748 cm^{-1} are assigned due to hydroxyl (O–H) groups stretching vibration, whereas the band at 2370 cm^{-1} is assigned to the adsorbed CO_2 gas. The small peaks between 2400 and 3000 cm^{-1} arise due to the C-H stretching vibration of alkane groups. The peaks around the region 1633–1554 cm^{-1} indicate H–O-H bending vibration and show the presence of the C = O amide group. The strong absorption band at 510 and 550 cm^{-1} are attributed to the Zn–O vibrations. In the case of Fig. 2b, the characteristic peak at 512 and 583 cm^{-1} is due to the Zn–O vibrations. The adsorption band at 624 cm^{-1} can be attributed to the acetate anions. The two characteristic bands at 1311and 1517 cm^{-1} attributed to asymmetric and symmetric stretching of the C = O bond in the acetate group. The adsorption band between 3176 and 3351 cm^{-1} is associated with the stretching mode of water. In Fig. 2c, the FTIR spectrum of ginger powder show several adsorption bands, which can be assigned to the hydroxyl group (3305 cm^{-1}), and the carbonyl group of amide (1639–1925 cm^{-1}). The small peak at 1380 cm^{-1} arises due to the presence of aromatic skeletal combined with C–H. The small band at 1044 cm^{-1} is attributed to the C–C bond's amino acid and stretching vibrations.

Table 1 Lattice parameters, unit cell volume, crystallite size, lattice strain, Rp, Rwp, Rexp, and goodness of fit ($\chi 2$) of green synthesized ZnO NPs

Lattice constant (Å)	Unit cell Vol (Å^3)	Atomic Positions			R-factors (%)		GoF (χ^2)	Bond Angle (degree)		Bond Length (Å)		Crystallite (nm)	Lattice-strain × 10^{-3}
a = b 3.2579	47.980	X	C	0.3333	R_p	14	2.50	O_a-Zn-O_a	O_b-Zn-O_b	Zn-O_a	Zn-O_b	31	2.518
c 5.220			O	0.3333	R_{exp}	7.19		108.4059	110.5152	1.97863	1.97738		
		Y	Zn	0.6667	R_{wp}	12.2							
			O	0.6667	R_f	1.09							
		Z	Zn	0.0129	R_{Bragg}	1.69							
			O	0.3750									

Field emission scanning electron microscope (FE-SEM) analysis

The surface morphology of the synthesized ZnO NPs by ginger rhizome extract was examined using SEM, as shown in Fig. 3a. The photos revealed the flaks type morphology with the small-nucleated particles on the surface. The phytochemical compounds found in the ginger rhizome extract work as a reducing and stabilizing agent so that particles have a facing surface. However, the material synthesis that occurs in liquid media is responsible for the high reaction rate and nucleation in the nanostructure. OH, ions act as binders between particles in liquid media, facilitating the self-assembly process that results in mesocrystals. According to the non-classical theory of crystallization, internal crystal symmetry is independent of the outer surface morphology of the grains (Ravinder and Reddy 1999). The alignment of nanocrystals in a typical crystallographic assembly that forms a particle with any external type regardless of unit cell geometry has been known as mesocrystal (Chae et al. 2012). The particle sizes distribution of the ZnO is shown in the inset particle size distribution (Fig. 3a). Figure 3b, c. Ionic distribution of zinc and oxygen. The transparency of ZnO crystal formation and uniform distribution of Zn and O atoms in the crystal was confirmed using Energy Dispersive X-ray (EDX), as shown in Fig. 3d. The results revealed that the Zn and O elements had the expected stoichiometry, demonstrating the efficacy of the synthesis method used. Zn and O are the sample's main constituents, and there were no impurity peaks, indicating that the samples were pure. The peak corresponding to elemental carbon may be due to the carbon tape used in SEM/EDX micrograph study.

Figure 4 HR-TEM images show that the well-defined lattice fringes resemble the crystallographic planes. The

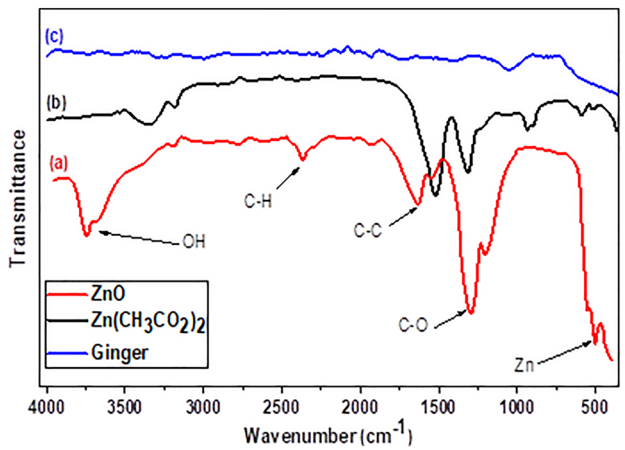

Fig. 2 FT-IR spectra of **a** Zinc Oxide, **b** Zinc Acetate, and **c** Ginger powder

average values corresponding to the interplanar spacing of crystallographic planes are equal to 0.71 nm. The interplanar spacing is comparable to the d-spacing calculated using XRD, i.e., 0.68 nm. Therefore, the interatomic analysis using both techniques, i.e., XRD and HR-TE, ensures that ZnO NPs are crystalline.

Ultraviolet–visible (UV) spectroscopy

The optical properties of ZnO NPs were investigated using the diffuse reflectance mode (DRS) UV–visible spectrum in 200–600 nm (Fig. 5). At 376.5 nm, the ZnO NPs display an absorption edge. The Kubelka–Munk equation (Eq. 2) calculates the band difference's energy (Eg). Tauc relation formed the relationship between Eg and photons (h) (Ahmed et al. 2015; Baykal et al. 2014). The difference in energies between photons (h) and Eg, as shown in Eq. 2 (Davis and Mott 1970), influences the frequency of optical absorption.

$$(\alpha h\nu)^{1/n} = A\left(h\nu - E_g\right) \tag{2}$$

In the above equation, h is the Planck constant, α is the absorption coefficient, ν is the light frequency, Eg is the bandgap, and A is the proportionality constant.

The bandgap values for ZnO NPs were 3.21 eV by plotting $(\alpha h\nu)^2$ verses $h\nu$ and extrapolating a straight line onto the X-axis. As shown in the inset tau map, the value of n indicates which absorption process is involved in the sample, with n = 2 indicating indirect bandgap transitions and n = 1/2 showing direct bandgap transitions (Kumar et al. 2018) (inset of Fig. 5). The absorption band appeared at 376.5 nm in Fig. 5; Eq. (2) used to calculate the band difference, which was 3.29 eV. The small particle size of the synthesized ZnO NPs is most likely to blame for the wideband difference. According to previous studies, the optical band gap of ZnO NPs ranges between 3.18 and 3.34 eV. The optical bandgap of the green synthesized ZnO NPs was 3.21 eV in the current analysis, with a blue shift from 3.16 to 3.22 eV. The blue shift in the band difference is due to the Burstein-Moss effect (Fifere et al. 2018). This effect states that the Fermi level's location is determined by the concentration of free electrons in the conduction band. The energy band difference is related to electron excitation from the valence band to the Fermi level. As a result, a Fermi level on the conduction band causes a widening of the energy band, referred to as a "blue shift."

Insecticidal efficacy of green synthesized ZnO NPs on the larva of *S. litura*

The effect of ZnO NPs on the mortality of *S. litura* was investigated at various concentrations. As concentrations and

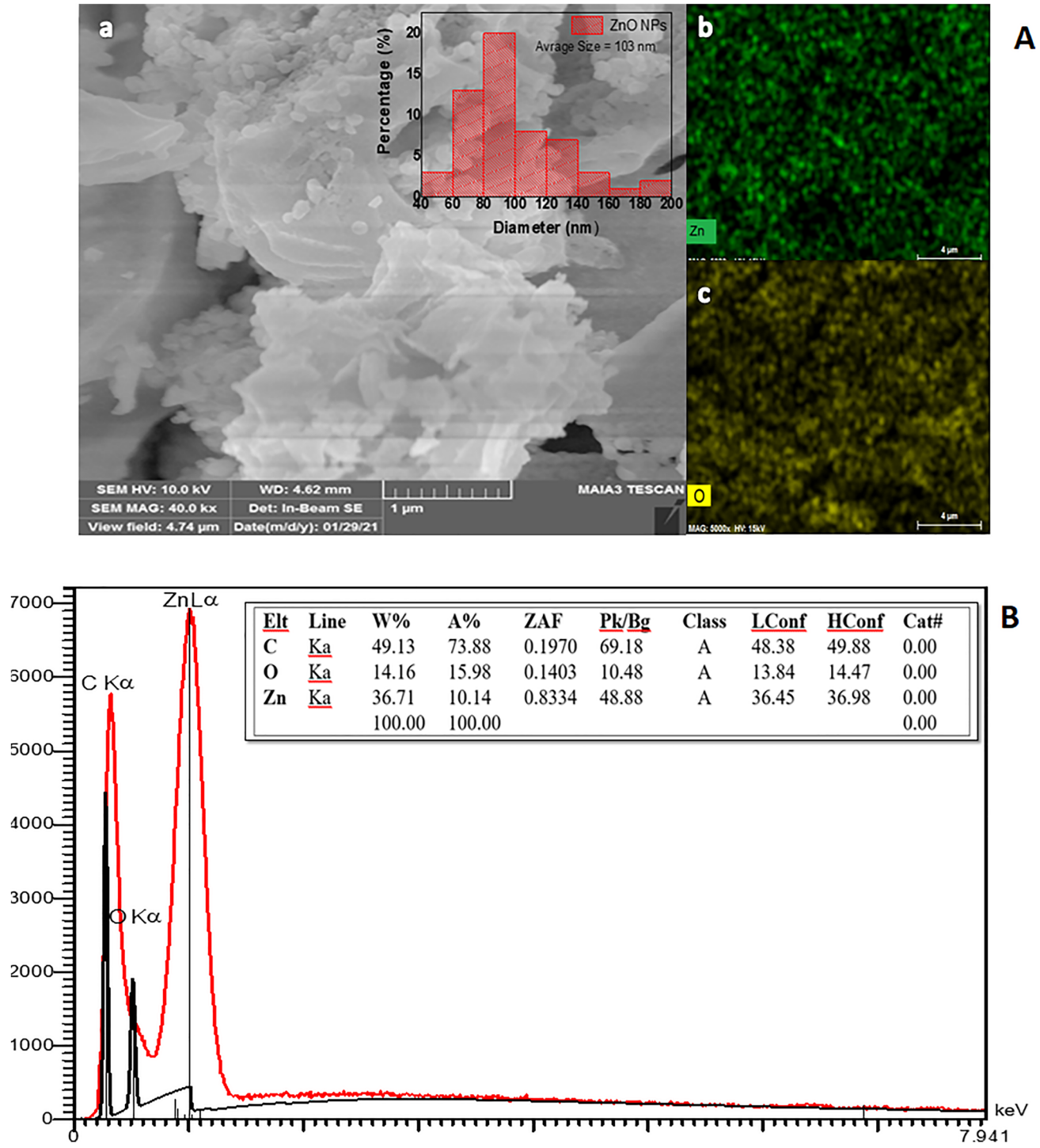

Elt	Line	W%	A%	ZAF	Pk/Bg	Class	LConf	HConf	Cat#
C	Ka	49.13	73.88	0.1970	69.18	A	48.38	49.88	0.00
O	Ka	14.16	15.98	0.1403	10.48	A	13.84	14.47	0.00
Zn	Ka	36.71	10.14	0.8334	48.88	A	36.45	36.98	0.00
		100.00	100.00						0.00

Fig. 3 **a** FE-SEM image (inset particle size distribution plot) **b** and **c** Ionic distribution of Zn and O **d** Energy Dispersive X-ray (EDX) of green synthesized ZnO NP prepared from *Z officinale* rhizome extract

the number of days after treatment increased, so did mortality (Table 2, Fig. 6). The maximum percent larval mortality for the 3rd instar larvae of *S. litura* was recorded at 500 ppm concentration (100%) after 144 h of exposure. At the lowest dose, i.e., 100 ppm, no mortality was observed after 24 h of treatment. With the increase in dose to 200 ppm, the larval mortality ranged from 4.67% to 40% after 24–120 h of exposure. Maximum mortality of 53.33% was observed after 144 h at this concentration. At 300 ppm concentration, the highest mortality of 76.67% was observed after 144 h

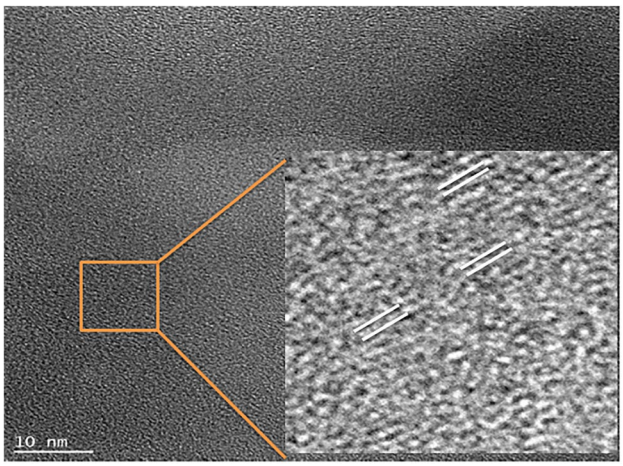

Fig. 4 HR-TEM image of green synthesized ZnO NPs prepared from *Z. officinale* rhizome extract

of treatment, whereas minimum mortality of 13.33% was observed after 24 h of treatment. It was observed that in all the treatments with the increase in time, the larval mortality also increased. The larval mortality of 60% and 70% were observed after 96 and 120 h, respectively, at this concentration. Maximum mortality of 80% was observed at this concentration after exposure of 144 h. At the highest concentration (500 ppm), the mortality observed was highest (30%) after 24 h of exposure, and 100% mortality was observed after 144 h. All the treatments were found superior over control. Thiamethoxam (0.5 mg/l) was used as a control. 24% mortality was observed after 24 h, and the highest mortality of 94.66% was observed after 144 h of treatment. Larval mortality after treatment with different concentrations of ZnO NPs and thiamethoxam increases dose-dependent. The LC_{50}value for ZnO NPs on *S. Litura* was calculated to be 232.34 ppm, as given in Table 4. Flow chart of insecticidal applications of ZnONP against Larvae of *S. litura* and adults of *M. euphorbiae* is shown in Scheme 2.

Similar results were obtained by Wazid et al. (2018), who studied the effect of Zinc oxide green nanoparticles (ZnO) on *Callosobruchus analysis* (Fabricius). The data from different zinc oxide green nanoparticles (250, 500, 750, 1000, 1250, and 1500 ppm) showed that adult mortality increased as the concentration and exposure time increased (percent). Among the various concentrations, 1500 ppm zinc oxide nanoparticle was superior, with the highest mortality rate. Jameel et al. (2020) reported the synergistic effect of the green synthesized ZnO NPs on *S. litura* 4th instar larvae (Lepidoptera: Noctuidae). These larvae were given ZnO NPs mixed with thiamethoxam (1090 mg/L) and thiamethoxam-impregnated castor leaves. In the experiment, there was a 27% rise in larval mortality, a malformation in pupae and adults, overdue emergence, and decreased fecundity and fertility.

Insecticidal efficacy of green synthesized ZnO NPs on *M. euphorbiae*

The effect of ZnO NPs on the mortality of *M. euphorbiae* was investigated at various concentrations. After 144 h of treatment, it was found that 100 percent mortality was observed at 500 ppm concentration. The lowest mortality (5.67%) was observed at 100 ppm concentration after 24 h of exposure. At 100 ppm concentration of ZnO NPs, the mortality ranged from 5.67%- to 44.33% after 24- 120 h. The highest mortality of 56.67% was observed after 144 h of the exposure period.

When the dose increased to 200 ppm, the mortality observed was 23.33%, 34.33%, 46.33%, 56.33%, and 63.33% after 24, 48, 72, 96, and 120 h, respectively. Maximum mortality of 73.33% was observed after 144 h of the exposure period. The highest mortality observed was 83.33% after 144 h at 300 ppm concentration. When adults of the aphid were treated with 400 ppm of ZnO NPs, the mortality recorded was 46.67%, 56.67%, 66.67%, 76.67%, and 86.67% after 24, 48, 72, 96, and 120 h, respectively. Maximum mortality of 93.33% was observed at this concentration after an exposure period of 144 h. The maximum mortality of 100% was observed @ 500 ppm concentration after 144 h of the treatment (Table 3, (Fig. 7)). Imidacloprid (0.5 ml/l) was used as a control in this experiment. 32% mortality was observed after 24 h, and the highest mortality of 93.33% was observed after 144 h of treatment. The LC_{50}value for ZnO NPs on *M. euphorbiae* was 124.81 ppm, as given in Table 4.

The present study aimed to determine the insecticidal effect of ZnO NPs on *S. litura* and *M. euphorbiae*. These pests have mainly been managed by using synthetic pesticides and a few biopesticides for many years. However, using these synthetic pesticides has damaged the environment and caused resistance to insecticides (Rajula et al. 2020). For that reason, research is being conducted on alternatives that can effectively manage this insect and are also safe for the environment. ZnO NPs have proved to be a promising source of safe insecticides yet effective in controlling *S. litura* and *M. euphorbiae*. Also, it has been observed that it can manage several other insect pests at environmentally friendly and low dosages of about 700 mg $mL-1$ had the highest insect mortality effect. Also, when leaves infested by *Aphis nerii* were dipped into various concentrations of ZnO NPs, there was a significant effect on their development (Rouhani et al. 2012). Similar results were obtained by Wazid et al. (2018), who studied the effect of Zinc oxide green synthesized nanoparticles (ZnO) on *Callosobruchus analis* (Fabricius). The data from the different concentrations

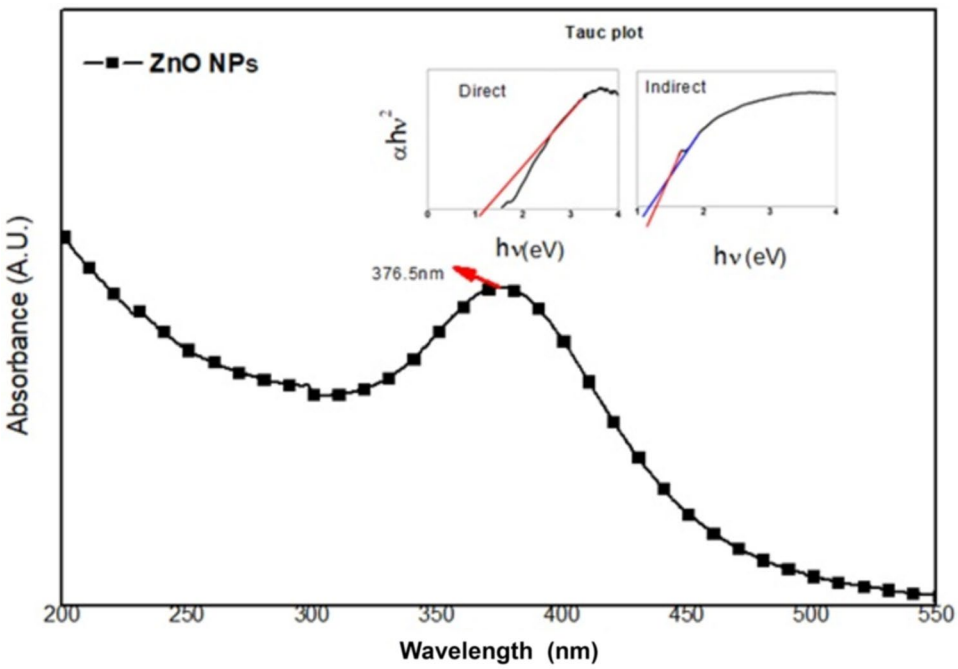

Fig. 5 UV–visible spectrum of green synthesized ZnO NPs prepared from *Z. officinale* rhizome extract

of ZnO NPs showed that adult mortality increased as the concentration and exposure time increased. Among the various concentrations, 1500 ppm zinc oxide nanoparticle was superior, with the highest mortality rate. (Jameel et al. 2020) reported the synergistic effect of the green synthesized ZnO NPs on *S. litura* 4th instar larvae (Lepidoptera: Noctuidae). These larvae were given ZnO NPs mixed with thiamethoxam and thiamethoxam-impregnated castor leaves. In the experiment, there was a 27% rise in larval mortality, a malformation in pupae and adults, overdue emergence, and decreased

Table 2 Efficacy of ZnO NPs against 3rdinstar larvae of *S. Litura*

Concentration	Corrected % mortality after hours					
	24	48	72	96	120	144
100 ppm	0.00 (0.00)	3.67 (6.28)	9.67 (16.84)	17.67 (20.98)	30.67 (37.21)	36.33 (40.90)
200 ppm	4.67 (8.28)	10.67 (13.84)	20.00 (23.19)	36.67 (37.21)	40.00 (44.98)	53.33 (56.75)
300 ppm	13.33 (21.13)	23.33 (28.76)	53.33 (57.20)	60.00 (50.83)	70.00 (56.97)	76.67 (61.19)
400 ppm	20.00 (26.55)	30.00 (32.98)	40.00 (39.13)	70.00 (56.97)	73.33 (58.98)	80.00 (63.90)
500 ppm	30.00 (33.19)	36.67 (37.21)	63.33 (52.75)	83.33 (66.11)	93.33 (77.69)	100 (90.00)
Thiamethoxam (0.5 mg/l)	24.00 (28.63)	32.67 (35.01)	46.66 (46.82)	66.00 (68.82)	74.00 (64.76)	94.66 (95.94)

Values are the average of triplicates. Figures in the parenthesis are standard deviation

CD	(P=0.05)
Concentration (C)	=0.36
Time(T)	=0.36
C×T	=0.89

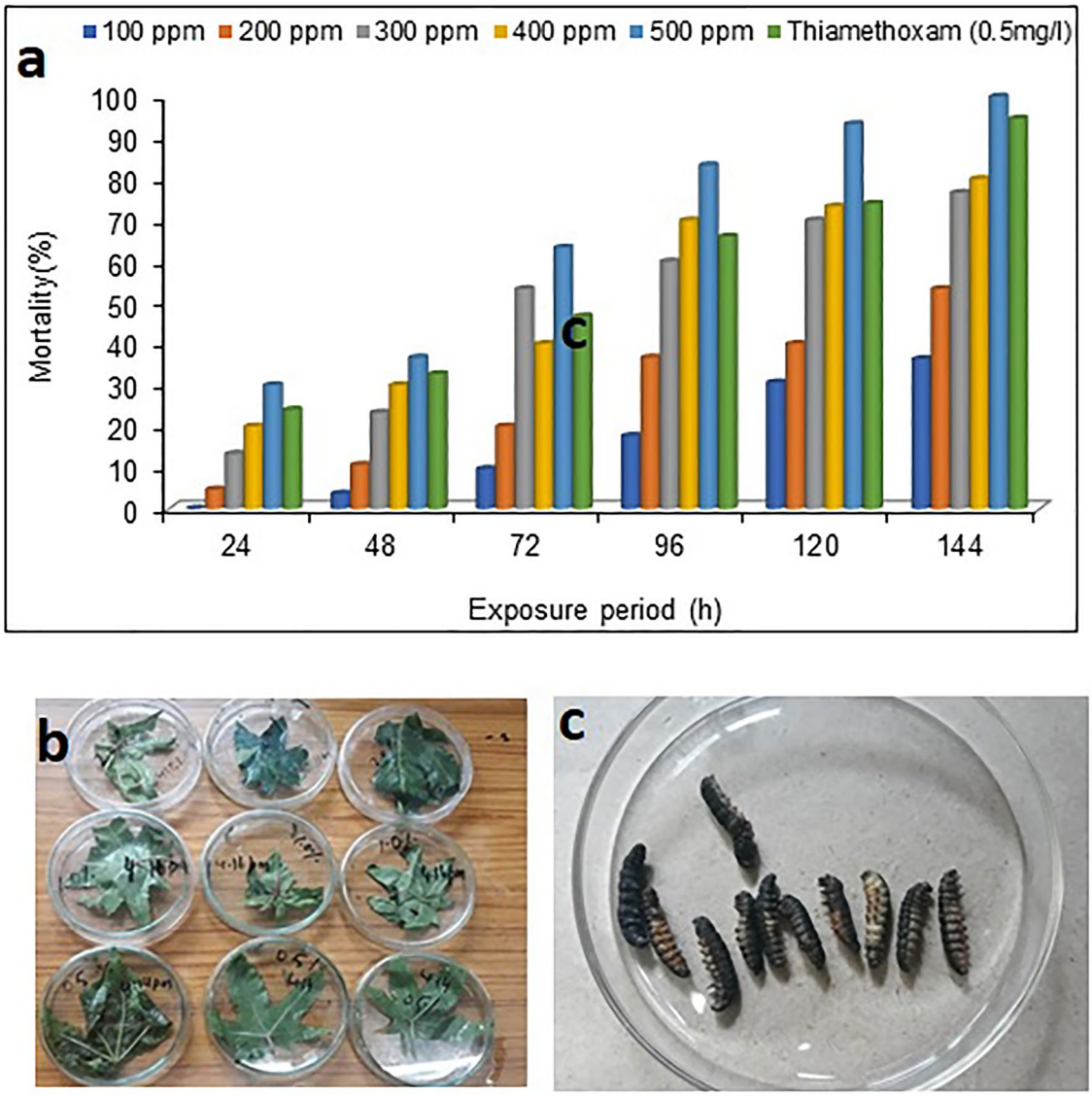

Fig. 6 **a** Efficacy of ZnO NPs against 3rdinstar larvae of *S. litura* **b** Larvae of *S. litura* affected by ZnO NPs on different time intervals **c** Larvae of *S. litura* affected by ZnO NPs

fecundity and fertility. These outcomes are similar to Lakshmi et al. (2020) report. They observed the effect of Zinc oxide nanoparticles at different concentrations on pulse beetle (*Callosobruchus maculatus*), and the highest mortality of 100% was recorded. Observations from the present study agree with other previous findings with different insects such as rice weevil, Sitophilus oryzae and whitefly, Trialeurodes vaporariorum where mortality was recorded due to exposure to ZnO NPs and showed high mortality rates up to 91% (Khooshe et al. 2016). A wide variety of nanoparticles are known to exert insecticidal properties of different insects/pests (Table 5).

Conclusion

The present work was performed to synthesize ZnO NPs by the green synthesis method. Ginger rhizome extract was used as a reducing and surfactant reagent. The developed ZnO nanoparticles were characterized for their structural and morphological study. ZnO NPs were produced at 50–100 nm and characterized by SEM and TEM studies. ZnO NPs exerted their toxicity against insects through the physical mode of action by absorption and abrasion of the protective wax layer on the cuticle of insects, causing the insects to lose water and die of desiccation. These insects are unlikely to develop any physiological resistance against these applied nanoparticles. ZnO NPs have the potential to

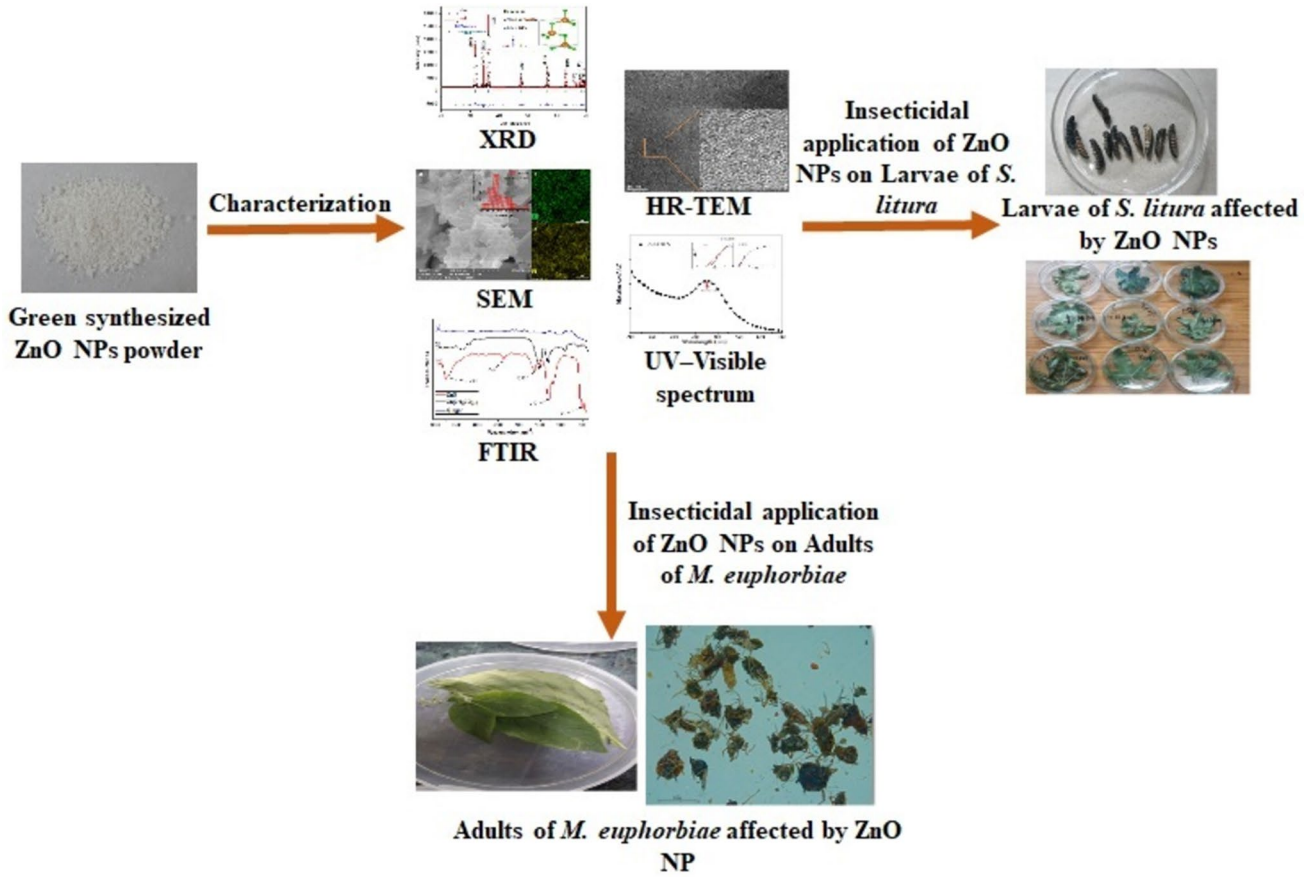

Scheme 2 Flow chart of insecticidal applications of ZnO NP against larvae of *S. litura* and adults of *M. euphorbiae*

Table 3 Efficacy of ZnO NPs against *M. euphorbiae*

Concentrations	Corrected % mortality after hours					
	24 h	48 h	72 h	96 h	120 h	144 h
100 ppm	5.67 (10.28)	14.00 (16.55)	20.00 (23.19)	33.33 (31.13)	44.33 (46.90)	56.67 (54.76)
200 ppm	23.33 (28.79)	34.33 (35.20)	46.33 (43.13)	56.33 (46.90)	63.33 (52.75)	73.33 (58.98)
300 ppm	36.67 (37.21)	46.67 (43.06)	56.67 (48.82)	63.33 (52.75)	73.33 (58.98)	83.33 (66.11)
400 ppm	46.67 (43.06)	56.67 (48.82)	66.67 (54.76)	76.67 (61.19)	86.67 (68.82)	93.33 (77.69)
500 ppm	56.67 (48.82)	66.67 (54.76)	76.67 (61.19)	86.67 (68.82)	96.67 (83.84)	100 (90.00)
Imidacloprid (0.5ml/l)	32.00 (34.03)	44.67 (41.67)	54.67 (47.81)	64.66 (54.15)	75.66 (62.25)	93.33 (89.50)

Figures in parentheses are arc sine transformed values:

CD	(P=0.05)
Concentration (C)	=0.2
Time(T)	=0.26
C×T	=0.64

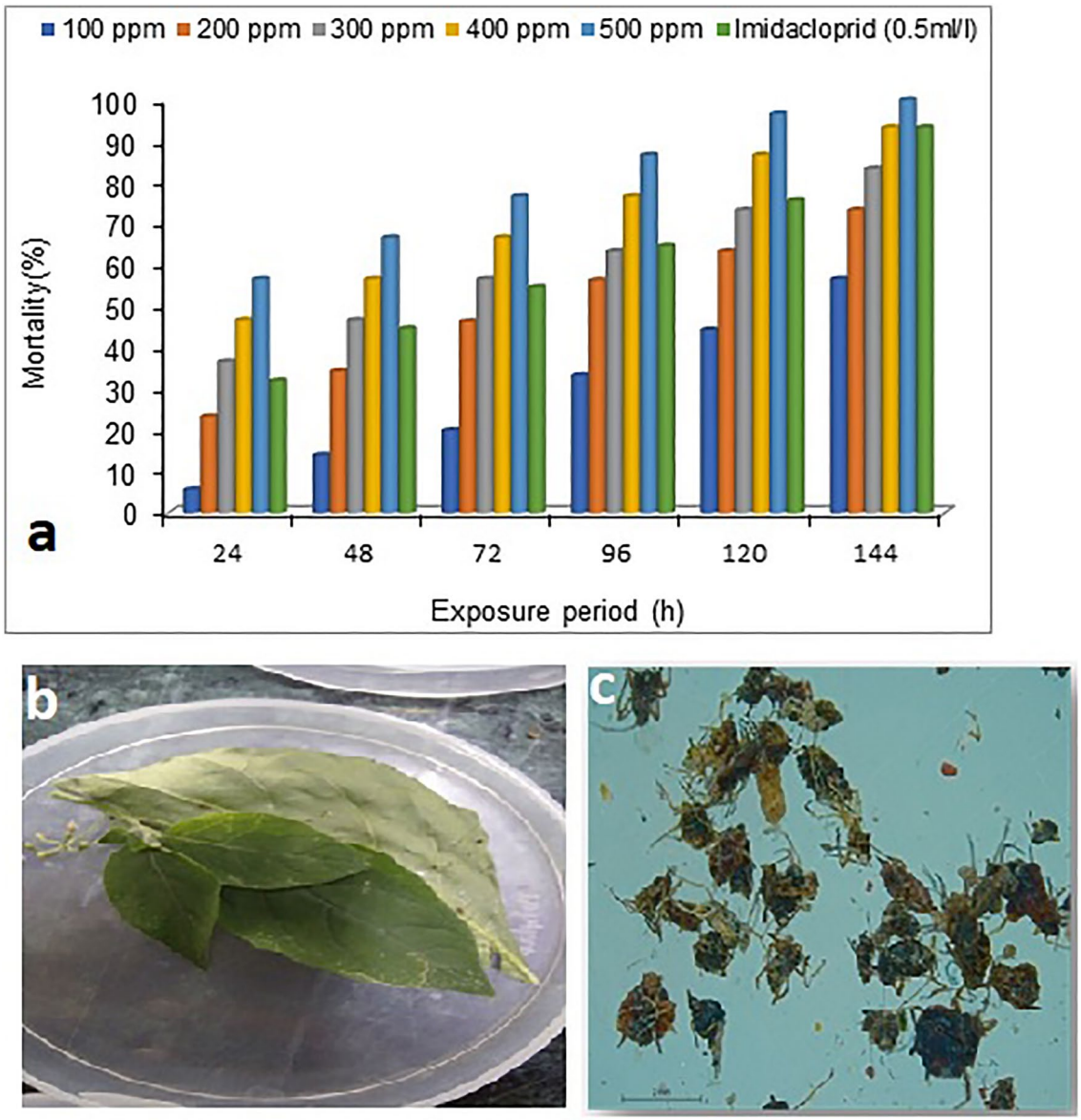

Fig. 7 **a** Efficacy of ZnO NPs against *M. Euphorbiae* **b** Adults of *M. euphorbiae* affected by ZnO NP **c** Microscopic image of M. euphorbiae affected by ZnO NPs

Table 4 Evaluation of ZnO NPs against 3.[rd]instar larvae of *S. Litura* and adult of *M. euphorbiae*

Test insect	Slope (±SE)	LC_{50}	Limits 95%	Chi square (χ^2)
S. litura	2.79 ± 0.90	232.34 ppm	235.42 – 287.67	1.28
M. *euphorbiae*	1.39 ± 0.80	124.81 ppm	113.21 – 165.32	0.90

be utilized as an alternative to more harmful insecticides in the control of *S. litura* (Tobacco cutworm) and *M. euphorbiae* (Potato aphid). Although, further research regarding the use of nanoparticles and their toxic effects on human health and the environmental impacts of employing ZnO NPs as pesticides are required. One evident advantage of using nanomaterials as insecticides is the low danger of insects acquiring resistance when used for a long time. The current study revealed the significant impacts of nanotechnology as an important part of any integrated pest management plan. 100% mortality was observed at 500 ppm concentration of ZnO NPs against *S. litura* and *M. euphorbiae* compared to commercial insecticides Thiamethoxam and Imidacloprid, respectively. Based on these studies, the results revealed

Table 5 Insecticidal properties of nanoparticles previously reported

Nanoparticles	Insects	Crops	References
DNA Tagged gold nanoparticles	*Spodoptera litura*	Tomato	Chakravarthy et al. (2012)
Nano-silica	*Spodoptera littoralis*	Tomato	El-bendary and El-Helaly (2013)
Silica nanoparticles	*Spodoptera littoralis*	Soybean	Borei et al. (2014)
Silver nanoparticles	*Helicoverpa armigera*	Cotton	Devi et al. (2014)
Silicon dioxide nanoparticles	*Rhyzopertha dominica* and *Tribolium confusum*	Stored grain	Ziaee and Ganji (2016)
Silver nanoparticles	*Macrosiphum rosae*	Rose	Bhattacharyya et al. (2016)
CuO nanoparticles	*Spodoptera littoralis*	Cotton	Shaker et al. (2016)
TiO_2 nanoparticles	*Spodoptera littoralis*	Cotton	Shaker et al. (2017)
CuO nanoparticles	*Tetranychus urticae*	Red bean	Dorri et al. (2018)
Cu-nanoparticles	*Prosopis solenopsis*	–	Leon-Jimenez et al. (2019)
ZnO nanoparticles	*Spodoptera frugiperda*	Maize	Pittarate et al. (2021)

that an increase in concentrations of the NPs increased the mortality in the insects. The attained results proved the proficiency of synthesized nanoparticles as an effective control agent. ZnO NPs have a subordinate chance of resistance with their insecticidal efficacy.

Acknowledgements The authors extend their appreciation to the Researchers supporting Project number (RSP-2021/98) King Saud University, Riyadh, Saudi Arabia and the Finnish Museum of Natural History, University of Helsinki PO Box 7 FI-00014 Helsinki, Finland for financial support.

Author contributions Conceptualization, Supervision; PK Methodology; TC Formal analysis; PK and ST Writing- review and editing; RZS; SSPP and AAA, Fund acquisition; PP and AAA. All the authors have agreed to the final version of the manuscript.

Funding This work was funded by The Researchers supporting Project number (RSP-2021/98) King Saud University, Riyadh, Saudi Arabia and The Finnish Museum of Natural History, the University of Helsinki, P.O. Box 7 FI-00014 Helsinki, Finland.

Declarations

Conflict of interest The authors declare that the research was conducted without any commercial or financial relationships that could be construed as a potential conflict of interest.

References

Abbott WS (1925) Methods for computing the effectiveness of insecticides. J of Econ Entomol 18:265–267

Ahmed AI, Siddig MA, Mirghni AA, Omer MI, Elbadawi AA (2015) Structural and optical properties of $Mg_{1-x}Zn_xFe_2O_4$ nanoferrites synthesized using co-precipitation method. Adv Nanopart 4:45

Arumugam G, Velayutham V, Shanmugavel S, Sundaram J (2016) Efficacy of nanostructured silica as a stored pulse protector against the infestation of bruchid beetle, *Callosobruchus maculatus* (Coleoptera: Bruchidae). Appl Nanosci 6:445–450

Baykal A, Guner S, Demir A, Esir S, Genç F (2014) Effect of zinc substitution on magneto-optical properties of $Mn_{1-x}Zn_xFe_2O_4/SiO_2$ nanocomposites. Ceram Int 40:13401–13408

Bhardwaj AK, Sundaram S, Yadav KK, Srivastav AL (2021) An overview of silver nano-particles as promising materials for water disinfection. Environ Technol Innov 23:101721

Bhattacharyya A, Bhaumik A, Rani PU, Mandal S, Epidi TT (2010) Nano-particles-A recent approach to insect pest control. Afr J Biotechnol 9:3489–3493

Bhattacharyya A, Prasad R, Buhroo AA, Duraisamy P, Yousuf I, Umadevi M, Bindhu MR, Govindarajan M, Khanday AL (2016) One-pot fabrication and characterization of silver nanoparticles using *Solanum lycopersicum*: an eco-friendly and potent control tool against rose Aphid *Macrosiphum rosae*. J Nanosci. https://doi.org/10.1155/2016/4679410

Borie HA, El-Samahy MF, Galal OA, Thabet AF (2014) The efficiency of silica nanoparticles in control cotton leafworm, *S. littoralis* (Lepidoptera :Noctuidae) in soybean plants under laboratory conditions. Glob J Agric Food Safety Sci 1:161–168

Chae SY, Yadav JB, Joo OS (2012) Electrospray-deposited nickel ferrite thin film electrode for hydrogen production in PV-assisted water electrolysis system. Int J Energy Res 36:1044–1050

Chakravarthy AK, Bhattacharyya A, Shashank PR, Epidi TT, Doddabasappa B, Mandal SK (2012) DNA-tagged nano gold: a new tool for the control of the armyworm, *Spodoptera litura Fab*. (Lepidoptera: Noctuidae). Afr J Biotechnol 11(38):9295–9301

Cuong HN, Pansambal S, Ghotekar S, Oza R, Hai NTT, Viet NM, Nguyen VH (2022) New frontiers in the plant extract mediated biosynthesis of copper oxide (CuO) nanoparticles and their potential applications: a review. Environ Res 203:111858

Dabhane H, Ghotekar S, Tambade P, Pansambal S, Murthy HA, Oza R, Medhane V (2021) A review on environmentally benevolent synthesis of Cds nanoparticle and there applications. Environ Chem Ecotoxicol 3:209–219

Davis E, Mott N (1970) Conduction in non-crystalline systems V. conductivity, optical absorption and photoconductivity in amorphous semiconductors. Philos Mag 22:0903–0922

Devi GD, Murugan K, Selvam CP (2014) Green synthesis of silver nanoparticles using *Euphorbia hirta* (Euphorbiaceae) leaf extract against crop pest of cotton bollworm, *Helicoverpa armigera* (Lepidoptera: Noctuidae). J Biopest 7:54

Donmez S (2020) Green Synthesis of zinc oxide nanoparticles using *Zingiber officinale* root extract and their applications in glucose biosensor. El-Cezeri J Sci Eng 7:1191–1200

Dorri HR, Khaghani S, Moghadam A, Ghanbari D, Bihamta MR (2018) The effect of copper nano-capsules on the control of two spotted spider mite (Tetranychus urticae). J Nanostruct 8(3):316–332

El-bendary HM, El-Helaly AA (2013) First record nanotechnology in agricultural: silica nanoparticles a potential new insecticide for pest control. App Sci Rep 4(3):241–246

Fifere N, Airinei A, Timpu D, Rotaru A, Sacarescu L, Ursu L (2018) New insights into structural and magnetic properties of Ce doped ZnO nanoparticles. J Alloys Compd 757:60–69

Ghotekar S, Pansambal S, Bilal M, Pingale SS, Oza R (2021) Environmentally friendly synthesis of Cr2O3 nanoparticles: characterization, applications and future perspective ─a review. Case Stud Chem Environ Eng 3:100089

Jabborova D, Annapurna K, Fayzullaeva M, Sulaymonov K, Kadirova D, Jabbarova Z, Sayyed RZ (2020) Isolation and characterization of endophytic bacteria from ginger (*Zingiber officinale* Rosc). Ann Phytomed 9(1):116–121

Jabborova D, Sayyed RZ, Azimov A, Jabbarov Z, Matchanov A, Enakiev Y, Baazeem A, Sabagh AE (2021) Danish S, Datta R. Impact of mineral fertilizers on mineral nutrients in the ginger rhizome and on soil enzymes activities and soil properties. Saudi J of Biol Sci 28:5268–5274. https://doi.org/10.1016/j.sjbs.2021.05.037

Jameel M, Shoeb M, Khan MT, Ullah R, Mobin M, Farooqi MK, Adnan SM (2020) Enhanced insecticidal activity of thiamethoxam by zinc oxide nanoparticles: a novel nanotechnology approach for pest control. ACS Omega 5:1607–1615

Janaki AC, Sailatha E, Gunasekaran S (2015) Synthesis, characteristics and antimicrobial activity of ZnO nanoparticles. Spectrochim Acta a: Mol Biomol Spectrosc 144:17–22

Kapadia C, Lokhandwala F, Patel P, Elesawy BH, Sayyed RZ, Alhazmi A, Haque S, Datta R (2021) Nanoparticles combined with cefixime as an effective synergistic strategy against *Salmonella Enteric typhi*. Saudi J of Biol Sci 28:4164–4172. https://doi.org/10.1016/j.sjbs.2021.05.032

Kashid Y, Ghotekar S, Bilal M, Pansambal S, Oza R, Varma RS, Nguyen VH, Murthy HA, Mane D (2022) Bio-inspired sustainable synthesis of silver chloride nanoparticles and there prominent applications. J Indian Chem Soc 99:100335

Kausar R, Shaheen MA, Maqbool Q, Naz S, Nazar M, Abbas F, Shams MF (2016) Facile biosynthesis of Ag-NPs using Otostegia limbata plant extract: physical characterization and auspicious biological activities. AIP Adv 6(9):095203

Khooshe-Bast Z, Sahebzadeh N, Ghaffari-Moghaddam M, Mirshekar A (2016) Insecticidal effects of zinc oxide nanoparticles and *Beauveria bassiana* TS11 on *Trialeurodes vaporariorum* (Westwood, 1856)(Hemiptera: Aleyrodidae). Acta Agric Acta Slov 107:299–309

Kranthi KR, Jadhav D, Wanjari R, Kranthi S, Russell D (2001) Pyrethroid resistance and mechanisms of resistance in field strains of *Helicoverpa armigera* (Lepidoptera: Noctuidae). J Econ Entomol 94:253–263

Kumar S, Shandilya M, Thakur S, Thakur N (2018) Structural, optical, and photoluminescence properties of K 0.5 Na 0.5 NbO 3 ceramics synthesized by sol–gel reaction method. J Solgel Sci Technol 88:646–653

Kumari P, Rai R, Kholkin A (2015) Influence of BiFeTaO3 addition on the electrical properties of Na0. 4725K0. 4725Li0. 055NbO3 ceramics system using impedance spectroscopy. J Alloys Compd 637:203–212

Lakshmi SJ, Roopa BRS, Sharanagouda HCTR, Sushila N (2020) Effect of zinc oxide nanoparticles on pulse beetle (*Callosobruchus maculatus*)(Col.: Chrysomelidae) in greengram. J Entomol Zool Stud 8:297–300

Leon JE, Valdez SB, Gonzalez MD, Tzintzun CO (2019) Síntesis y actividad insecticida de nanopartículas de Cu de Prosopis juliflora (Sw) DC y Pluchea sericea (Nutt.) sobre Phenacoccus solenopsis Tinsley (Hemiptera: Pseudococcidae). Revista de la Sociedad Entomológica Argentina, 78(2): 1–10

Malaikozhundan B, Vinodhini J, Kalanjiam MAR, Vinotha V, Palanisamy S, Vaseeharan VS, Mariyappan A (2020) High synergistic antibacterial, antibiofilm, the antidiabetic and antimetabolic activity of *Withania somnifera* leaf extract-assisted zinc oxide nanoparticle. Bioprocess Biosyst 43:1533–1547

Nayeri FD, Mafakheri S, Mirhosseini M, Sayyed R (2021) Phytomediated silver nanoparticles via Melissa officinalis aqueous and methanolic extracts: synthesis characterization and biological properties against infectious bacterial strains. Intl J Adv Biol Biomed Res 9(3):270–285. https://doi.org/10.22034/ijabbr.2021.525079.1349

Pandit C, Roy A, Ghotekar S, Khusro A, Islam MN, Emran TB, Lam SE, Khandaker MU, Bradley DA (2022) Biological agents for the synthesis of nanoparticles and there applications. J King Saud Univ Sci 34:101869

Pittarate S, Rajula J, Rahman A, Vivekanandhan P, Thungrabeab M, Mekchay S, Krutmuang P (2021) Insecticidal effects of zinc oxide nanoparticles against *Spodoptera frugiperda* under laboratory conditions. Insects 12:1017

Raafat M, El-Sayed AS, El-Sayed MT (2021) Biosynthesis and antimycotoxigenic activity of *Zingiber officinale* Roscoe-derived, metal nanoparticles. Molecules 26:2290

Ragaei M, Sabry AKH (2014) Nanotechnology for insect pest control. Int J Science Environ Technol 3:528–545

Rai M, Ingle A (2012) Role of nanotechnology in agriculture with special reference to the management of insect pests. Appl Microbiol Biotechnol 94:287–293

Rai R, Kumari P, Valente M (2015) Study the structural and magnetic properties of rare-earth ions (La and Gd) doped Ba0. 9575Ca0. 0025Ti0. 80685Mn0. 002475Nb0. 002475Zr0. 1782O3. (BCT-MNZ) ceramics. J Adv Dielectr 5:1520001

Rajula J, KrutmuangP, RA (2020) Entomopathogenic fungi in Southeast Asia and Africa and their possible adoption in biological control. Biol Control 151:104399

Ramanarayanan R, Bhabhina N, Dharsana M, Nivedita C, Sindhu S (2018) Green synthesis of zinc oxide nanoparticles using extract of *Averrhoa bilimbi* (L) and their photoelectrode applications. Mater Today 5:16472–16477

Rani L, Thapa K, Kanojia N, Sharma N, Singh S, Grewal A, Srivastav A, Kaushal J (2021) An extensive review on the consequences of chemical pesticides on human health and environment. J Clean Prod 283:124657

Ravinder D, Reddy AR (1999) Electrical transport properties of zinc-substituted manganese ferrites. Mater Lett 38:265–269

Rouhani M, Samih MA, Kalantari S (2012) Insecticide effect of silver and zinc nanoparticles against *Aphis nerii* Boyer De Fonscolombe (Hemiptera: Aphididae). Chil J Agric Res 72(4):590

Sajjad M, Ashfaq M, Suhail A, Akhtar S (2011) Screening of tomato genotypes for resistance to tomato fruit borer (*Helicoverpa armigera* Hubner) in Pakistan. Pak J Agric Sci 48:59–62

Schwartz VB, Thetiot F, Ritz S, Putz S, Choritz L, Lappas A, Forch R, Landfester K, Jonas U (2012) Antibacterial surface coatings from zinc oxide nanoparticles embedded in poly (n-isopropyl acrylamide) hydrogel surface layers. Adv Funct Mater 22:2376–2386

Shaker AM, Zaki AH, Abdel-Rahim EF, Khedr MH (2016) Novel CuO nanoparticles for pest management and pesticides photodegradation. Adv Environ Biol 10(12):274–283

Shaker AM, Zaki AH, Abdel-Rahim EFM, Khedr MH (2017) TiO2 nanoparticles as an effective nanopesticide for cotton leaf worm. Agric Eng Int: CIGR J 14:61–68

Sharon M, Choudhary AK, Kumar R (2010) Nanotechnology in agricultural diseases and food safety. J Phytol 16:2–4

Sirelkhatim A, Mahmud S, Seeni A, Kaus NHM, Ann LC, Bakhori SKM, Hasan H, Mohamad D (2015) Review on zinc oxide nanoparticles: antibacterial activity and toxicity mechanism. Nanomicro Let 7:219–242

Thakur S, Kaur M, Lim WF, Lal M (2020a) Fabrication, and characterization of electrospun ZnO nanofibers; antimicrobial assessment. Mater Lett 264:127279

Thakur S, Shandilya M, Thakur S, Sharma DK (2020b) Growth mechanism and characterization of CuO nanostructure as a potent antimicrobial agent. Surf Interf 20:100551

Thakur S, Shandilya M, Guleria G (2021) Appraisement of antimicrobial zinc oxide nanoparticles through *Cannabis jatropha* curcasa Alovera and *Tinospora cordifolia* leaves by green synthesis process. J Environ Chem Eng 9:104882

Vijayakumar S, Vaseeharan B, Sudhakaran R, Jeyakandan J, Ramasamy P, Sonawane A, Padhi A, Velusamy P, Anbu P, Faggio C (2019) Bioinspired zinc oxide nanoparticles using Lycopersicon esculentum for antimicrobial and anticancer applications. J Clust Sci 30:1465–1479

Wazid NW, Prabhuraj A, Naik R, Shakuntala N, Sharanagouda H (2018) Effect of biosynthesized zinc oxide green nanoparticles on pulse beetle, *Callosobruchus analis* (Coleoptera: Chrysomelidae). Int J Curr Microbiol Appl Sci 7:503–512

Wojnarowicz J, Chudoba T, Lojkowski W (2020) A review of microwave synthesis of zinc oxide nanomaterials: reactants, process parameters and morphologies. Nanomaterials 10:1086

Yu Y, Zhang J, Chen C, He C, Miao J, Li H, Chen J (2020) Effects of calcination temperature on physicochemical property and activity of CuSO4/TiO_2 ammonia-selective catalytic reduction catalysts. J Environ Sci 91:237–245

Ziaee M, Ganji Z (2016) Insecticidal efficacy of silica nanoparticles against *Rhyzopertha dominica* F. and Tribolium confusum Jacquelin du Val. J Plant Prot Res. 56(3):250